JOURNAL OF MODERN OPTICS, 1992, VOL. 39, NO. 2, 325–334

Motional sidebands in the microwave spectra of ions in an rf trap

V. ENDERS, PH. COURTEILLE, W. NEUHAUSER and R. BLATT

I. Institut für Experimentalphysik, Universität Hamburg, Jungiusstraße 9, D-2000 Hamburg, Germany

(*Received 8 July 1991; revision received 20 August 1991*)

Abstract. The atomic motion of an ion in an rf trap adds sidebands to the ion's hyperfine transitions, shifted and broadened by the space charge. Sidebands and carrier depend differently on the microwave polarization, which is determined by observing microwave spectra with the orientation of the dc magnetic field varied. This phenomenon is caused by dc amplitude and phase modulation of the microwave radiation that is partially reflected inside the trap.

Downloaded By: [Universisty of Sao Paulo] At: 21:45 3 March 2010

1. Introduction

Precision spectroscopy on clouds of trapped ions dates back more than two decades [1]. The application of tunable lasers as light sources in rf–optical double resonance arrangements has demonstrated both appreciable fluorescence signals and high spectral resolution [2]. The conditions which the trapping technique provides for the stored ions include (i) long times of interaction with the radiation fields, such that the ionic lines are not broadened by a finite transit time, and (ii) the absence of collisions with both walls and background gas.

Moreover, the first-order Doppler effect reduces to weak spectral sidebands in addition to an unshifted carrier as soon as the ions move, with spatial excursions smaller than half the wavelength of the radiation [3]. This condition holds for rf and microwave interaction with the trapped ions in most experiments. The largest remaining systematic frequency shifts, of the order of 10^{-12}, derive from the space charge in the ion cloud and from the second-order Doppler effect. The appreciable potential accuracy—which would still be increased, by cooling the ions, for example—was the motivation for demonstrations of standard clocks controlled by $^{199}Hg^+$, $^{9}Be^+$ and $^{171}Yb^+$ [4–6]. To this end, the shapes of the rf lines have to be known in full detail.

The subject of this paper is a study of the line shape of the 12·6 GHz hyperfine transition of some 10^6 $^{171}Yb^+$ ions in an rf or Paul trap, as detected by the excitation of the ion's fluorescence [7]. Of particular interest are the motional sidebands and their dependence on the direction and polarization of the applied microwave field, with respect to an external magnetic field. Under certain conditions motional sidebands are absent. In section 2 the ion motion in a Paul trap is briefly reviewed, and some features of ion clouds are described. The characteristics of $^{171}Yb^+$ are described in section 3, and the Zeeman structure of the transition is outlined. In section 4 we present the experiment and show various spectra; in particular, for the motional sidebands. The experimental results are discussed and interpreted in section 5.

0950–0340/92 $3·00 © 1992 Taylor & Francis Ltd.

2. Ion motion in a Paul trap

The superimposed ac and dc fields between the ring and the cap electrodes of a Paul trap generate the time-dependent potential [8]

$$\Phi(x, y, z) = -\frac{m\Omega^2}{16}(a_z - 2q_z \cos \Omega t)(r^2 - 2z^2), \tag{1}$$

with $r^2 = x^2 + y^2$ and

$$a_z = -2a_r = -\frac{8eU}{mr_0^2\Omega^2}, \qquad q_z = -2q_r = \frac{4eV}{mr_0^2\Omega^2},$$

where m denotes the ion's mass, e is the elementary charge, r_0 is the radius of the ring electrode, U and V are the applied dc and ac voltages, respectively, and $\Omega/2\pi$ is the driving frequency. The potential has cylindrical symmetry, and ideally the electrodes are shaped according to single-shelled and double-shelled hyperboloids. The equations of motion of an individual ion in the potential (1) are

$$\ddot{u} + (a_u - 2q_u \cos 2v)u = 0, \tag{2}$$

where $u = r, z$, $r^2 = x^2 + y^2$ and $v = \Omega t/2$. The solution of the Mathieu equation (2) can be approximated in the pseudopotential model as [8]

$$u(t) = u_0(1 + \beta_u/2 \cos \omega_u t) \cos(\Omega t + \varphi), \tag{3}$$

where $\omega_u = \beta_u/2\Omega$ and $\beta_u^2 = \beta_u^2(a_u, q_u) \simeq a_u + q_u^2/2$. This solution describes the ion motion in terms of a slow oscillation at the secular frequency $\omega_u (u = r, z)$ and a superimposed micromotion with the drive frequency Ω. The pseudopotential approximation is valid for parameters $|a_u| \ll q_u \ll 1$. For an ion cloud the Coulomb repulsion between the ions modifies the dynamics; it has been modelled in various ways [9–14]. The trapping potential (1) has to be modified by taking the space charge into account, which is represented by a Gaussian spatial distribution. In first order, this extension leads to an additional dc component of the potential which changes the parameter a by Δa, which can be evaluated from the space-charge distribution. Assuming the space charge uniformly distributed, one obtains [15]

$$\Delta a_z = -\frac{8}{3}\frac{e\rho_{sc}}{m\varepsilon_0\Omega^2}, \tag{4}$$

with the space charge density ρ_{sc} and the dielectric constant ε_0. Since the secular frequency ω_u sensitively depends on the potential parameter, we expect to observe two modifications: (1) the secular frequencies are down-shifted, since Δa_z is negative; (ii) the shift of potential caused by the space charge in the cloud spatially varies and makes the secular frequencies distributed. Hence, the observed motional sidebands, unlike the carrier, show a broad spectral distribution [11, 16].

3. The Yb^+ ion

Figure 1 shows the energy levels of $^{171}Yb^+$ which are relevant for the rf–optical double resonance. The ground state of $^{171}Yb^+$ is split by hyperfine interaction into two levels, $F = 0, 1$, of 12·64 GHz separation. Resonance excitation of the ions in the $6^2S_{1/2}$, $F = 1$ level, by laser radiation at 369·4 nm results in optically pumping the ions into the $6^2S_{1/2}$, $F = 0$ state, i.e. the detected fluorescence signal decreases.

Downloaded By: [University of Sao Paulo] At: 21:45 3 March 2010

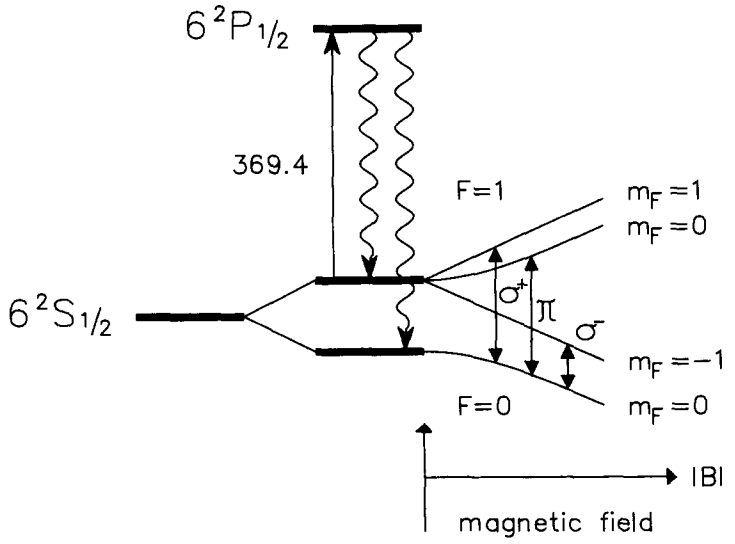

Figure 1. Optical pumping scheme and Zeeman levels of the ground state. The hfs splitting of the excited state is not shown.

Resonant microwave radiation at 12·6 GHz repopulates the $6^2S_{1/2}$, $F=1$ level, as indicated by increased fluorescence.

In an external magnetic field, the $F=1$ level Zeeman splits, and three resonances appear in the microwave spectrum (figure 1). The frequency of the $\sigma_\pm$ components depends linearly on the magnetic field, while the shift of the π component is quadratic. Thus, line broadening by field inhomogeneities is small only for the π component. This transition has been used for the control of an oscillator frequency [6].

The presence of sidebands requires Zeeman splitting larger than 5 μT for complete resolution of the components.

4. Experiment and results

The ion trap has hyperboloidic electrodes; the inner ring diameter is $2r_0=4$ cm, and the operating parameters are $V=600$ V, $U=11$ V and $\Omega/2\pi=460$ kHz. Three orthogonal pairs of Helmholtz coils compensate dc stray fields and the earths magnetic field to a few nT. This set-up also allows one to generate a magnetic field of any direction and with magnitude up to a few mT. Figure 2 shows a spectrum observed with the modulus of the magnetic field, $|\mathbf{B}|=7$ μT. The $\sigma_\pm$ components are much broader than the π component due to residual inhomogeneity of the magnetic field across the ion cloud: the respective widths are $\Delta(\sigma_\pm)\simeq 5$ kHz and $\Delta(\pi)\simeq 1{\cdot}2$ kHz, but we are able to resolve the π component with a 0·5 Hz linewidth [6]. Note the motional sidebands which show up to the left and right of each component. Their peaks indicate the mean secular frequency $\omega_{sc}/2\pi=15$ kHz, and the distribution of secular frequencies is about 10 kHz wide. From the trap parameters, we derive the (single ion) secular frequencies $\omega_z/2\pi=60$ kHz and $\omega_r/2\pi=38$ kHz. Both broadening and shift indicate the presence of space charge potential. The operating parameters are adjusted to get $\omega_r^s=\omega_z^s\equiv\omega_{sc}$ for the shifted secular frequencies. Then only two motional sidebands in the microwave spectrum

Downloaded By: [University of Sao Paulo] At: 21:45 3 March 2010

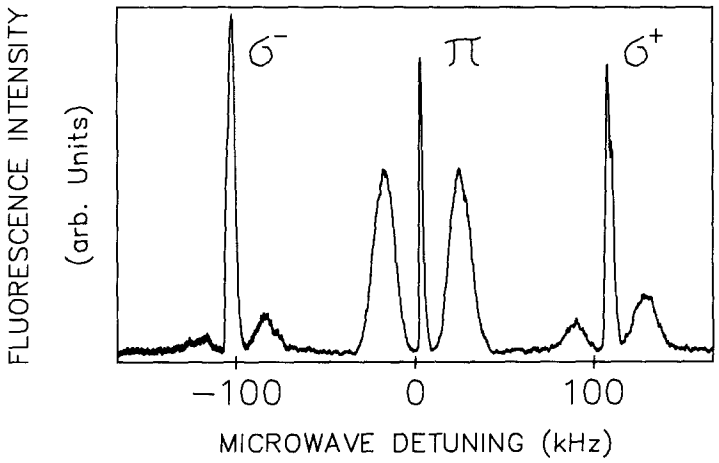

Figure 2. Spectrum of the hfs transition of $^{171}Yb^{+}$ showing the $\sigma_{\pm}$, π components with motional sidebands.

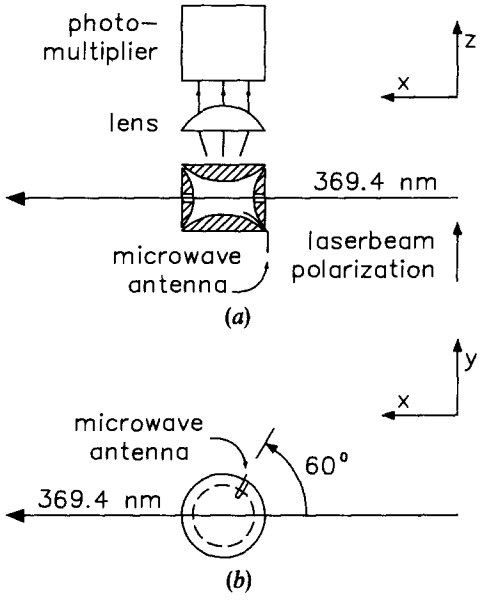

Figure 3. Experimental set-up: (*a*) the propagation and the polarization of the laser beam in the x–z plane; (*b*) the position of the microwave antenna viewed out of the z-direction.

are observed and the trapping potential modified by space charge is quasispherical. Modelling the space charge by a shift of the dc potential

$$\Delta a_z = \frac{4}{\Omega^2}(\omega_{sc}^2 - \omega_z^2),$$

we obtain $\Delta a_z = -0{\cdot}063$. From (4) we estimate the space-charge density in the trap to be $\rho_{sc}/e = 1{\cdot}9 \times 10^7\ \mathrm{cm}^{-3}$.

The microwave is emitted by a hairpin antenna placed in the gap between the ring electrode and the lower endcap and oriented at about 60° with respect to the x axis (see figure 3). Figure 4 shows microwave spectra at varying directions of the

Downloaded By: [Universisty of Sao Paulo] At: 21:45 3 March 2010

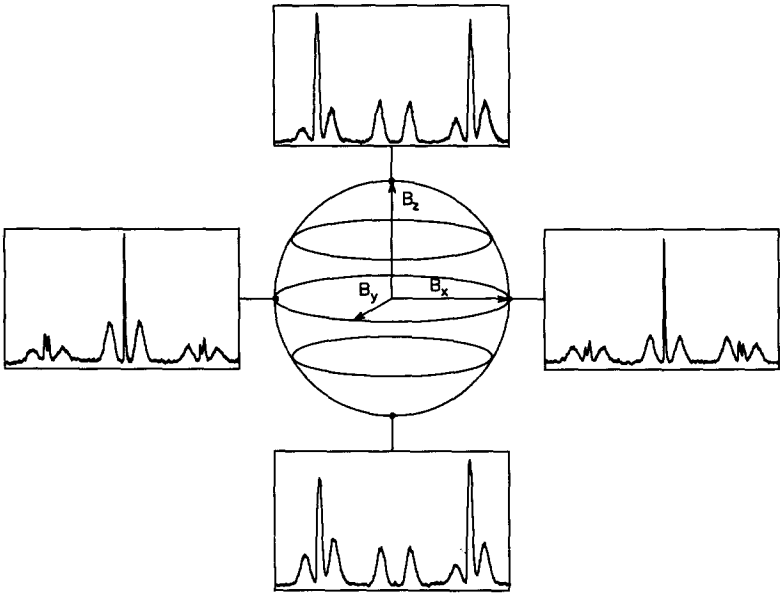

Figure 4. Spectra of the hfs transition components for various magnetic field orientations.

magnetic field vector and constant field modulus, where z is the trap axis of symmetry, and x the direction of light propagation. The sphere in figure 4 indicates the actual orientation of the magnetic field vector for the spectra.

The upper and lower spectra ($\mathbf{B}=|\mathbf{B}|(0,0,\pm 1)$) show no π component but maximum $\sigma_\pm$ components at the carrier frequencies, while the left and right spectra display opposite features. This observation proves that the microwave field is linearly polarized along the x direction. Note that the corresponding sidebands behave otherwise: they do not change except for a small asymmetry observed with the $\sigma_\pm$ components.

Inspection of the sidebands with $\mathbf{B}$ extending in the other direction reveals the π component to disappear when the magnetic field extends 45° or 225° with the z axis (see figure 5), i.e. with $\mathbf{B}\sim(\pm 1,0,\pm 1)$. When $\mathbf{B}$ extends orthogonally to these directions, the sideband amplitude of the π component is maximum and the sidebands of the σ components almost vanish.

5. Discussion

The microwave field emitted from the hairpin antenna is reflected from the stainless steel electrodes of the trap; hence, a standing wave is at least partially generated. Because of losses in the microwave cavity build-up from the trap's electrodes a travelling part of the microwave remains [17]. The distance between two neighbouring nodes or antinodes of the standing field is about 12 mm. Thus, the intensity of the microwave radiation acting on an ion cloud, with a diameter which has similar size, changes drastically along a single ion's trajectory. In the frame of reference moving with an ion the microwave field appears amplitude-modulated and corresponding sidebands are generated in the spectrum. Note that the secular frequency is position-dependent due to space charge, thus leading to the observed width of the motional sidebands. The travelling wave part appears phase modulated in this reference system. First, we investigate the influence of the standing wave part

Downloaded By: [University of Sao Paulo] At: 21:45 3 March 2010

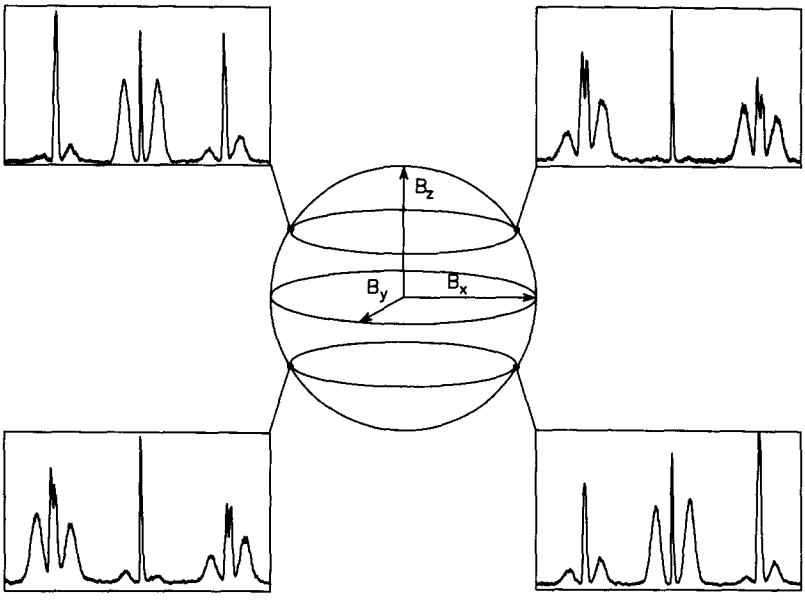

Figure 5. Spectra of the hfs transition components for magnetic field orientations at an angle of 45° with respect to the polarization axis.

on the line shape of the hfs transition. To explain the unexpected behaviour of the motional sidebands upon changing the magnetic field direction (see figure 5) we assume that the microwave polarization changes along an ion trajectory as well. Since the trap surfaces are of hyperbolic shape, polarization gradients over an area the size of the ion cloud are not unexpected.

We choose a coordinate system in the reference frame moving with an ion with axis (x_1, x_2, x_3), where x_3 is parallel to the Poynting vector of the microwave. Then the field amplitudes **E** and **H** are in the plane determined by x_1 and x_2. The observed hfs transitions are magnetic dipole transitions, and therefore we have to look at the magnetic field vector $\mathbf{H}(t)$ of the microwave.

For an ion oscillating in the standing wave, amplitude and polarization only change by moving along the direction parallel to the Poynting vector.

In our coordinate system we can describe these changes by splitting the field amplitude $\mathbf{H}(t)$ into two amplitude-modulated components $(H_1(t), H_2(t))$, pointing in the x_1 and x_2 direction, respectively. In the frame of reference oscillating with an ion in the x_3 direction at frequency Ω, the two components $H_1(t)$ and $H_2(t)$ show amplitude modulation with the modulation indices M and N:

$$\mathbf{H}(t) = (H_1(t), H_2(t)), \tag{5}$$

where

$$H_1(t) = H_{01}^{a}(1 + M\cos\Omega t)\exp(i\omega t)$$

and

$$H_2(t) = H_{02}^{a}(1 + N\cos(\Omega t + \varphi))\exp(i\omega t).$$

Downloaded By: [University of Sao Paulo] At: 21:45 3 March 2010

H^a_{0i}, $i=1,2$ are the amplitudes of each component, ω is the microwave frequency and φ denotes a possible phase shift in the modulation between the two components H_1 and H_2. Expanding (5) into Fourier components leads to

$$\mathbf{H}(t)=\begin{pmatrix}H^a_{01}\\H^a_{02}\end{pmatrix}\exp(i\omega t)+\begin{pmatrix}\frac{M}{2}H^a_{01}\\\frac{N}{2}H^a_{02}\exp(i\varphi)\end{pmatrix}\exp[(\omega+\Omega)t]$$
$$+\begin{pmatrix}\frac{M}{2}H^a_{01}\\\frac{N}{2}H^a_{02}\exp(i\varphi)\end{pmatrix}\exp[i(\omega-\Omega)t]. \tag{6}$$

Note that only in the case $N=M$ and $\varphi=0$ the polarization of carrier and sidebands are not different. In order to explain the observed behaviour of the motional sidebands (see figures 4 and 5) we have to choose $N=0$, $M=1$ and $|H^a_{01}|=|H^a_{02}|$, while H^a_{01} is pointing in the $(1,0,-1)$ direction and H^a_{02} in the $(1,0,1)$ direction. Hence, only one component (i.e. H^a_{01}) is affected by amplitude modulation:

$$\mathbf{H}(t)=\begin{pmatrix}H^a_{01}\\H^a_{02}\end{pmatrix}\exp(i\omega t)+\begin{pmatrix}\frac{M}{2}H^a_{01}\\0\end{pmatrix}\exp[i(\omega+\Omega)t]$$
$$+\begin{pmatrix}\frac{M}{2}H^a_{01}\\0\end{pmatrix}\exp[i(\omega-\Omega)t]. \tag{7}$$

In this case the polarization vectors of carrier and sidebands include an angle of 45°.

As mentioned above, the total microwave field in the trap is a superposition of a standing and a travelling wave. A travelling plane wave propagating in the x_3 direction occurs phase-modulated in the moving reference system, with modulation index P. For the components H^p_i, $i=1,2$, of the travelling wave with polarization in the x_1 and x_2 direction, respectively, we can write

$$H^p_i(t)=H^p_{0i}\exp(i\omega t+P\sin\Omega t)\qquad i=1,2. \tag{8}$$

Expanding (8) in terms of Bessel functions we obtain

$$H^p_i=H^p_{0i}[J_0(P)\exp(i\omega t)+J_1(P)\exp[i(\omega+\Omega)t]-J_1(P)\exp[i(\omega-\Omega)t]+\ldots]. \tag{9}$$

The index of modulation depends on the scalar product of the ion velocity amplitude $\mathbf{v}$ and the wavevector $\mathbf{k}_\omega$ of the microwave frequency. Looking at an ion with the mean velocity amplitude $\langle\mathbf{v}^2\rangle^{1/2}$ the index of modulation is given by

$$P=\frac{\langle\mathbf{v}^2\rangle^{1/2}}{3\Omega}k_\omega, \tag{10}$$

where k_ω denotes the wavenumber for the microwave transition and $\langle\mathbf{v}^2\rangle^{1/2}$ can be calculated from the mean kinetic energy $\overline{\langle E_{kin}\rangle}$ of an ion cloud's secular motion. The factor 1/3 appears by performing the scalar product. In the framework of dynamic models for ion clouds in Paul traps $\overline{\langle E_{kin}\rangle}$ can be estimated to be about 0·2 eV [10, 11]

Downloaded By: [University of Sao Paulo] At: 21:45 3 March 2010

and, therefore, $P=0{\cdot}1$. Thus, only first-order sidebands can be observed for the current trap parameters. In the moving reference system, equations (7) and (9) describe the total field acting upon an ion in the present trap:

$$\mathbf{H}(t)=\begin{pmatrix} H^{a}_{01}+H^{p}_{01}J_0(P) \\ H^{a}_{02}+H^{p}_{02}J_0(P) \end{pmatrix}\exp(i\omega t)+\begin{pmatrix} \frac{M}{2}H^{a}_{01}+H^{p}_{01}J_1(P) \\ H^{p}_{02}J_1(P) \end{pmatrix}\exp[i(\omega+\Omega)t]$$
$$+\begin{pmatrix} \frac{M}{2}H^{a}_{01}-H^{p}_{01}J_1(P) \\ -H^{p}_{02}J_1(P) \end{pmatrix}\exp[i(\omega-\Omega)t]. \tag{11}$$

The amplitudes of the two sidebands generated by amplitude modulation is influenced by phase modulation in different ways. One sideband is enlarged while the other is reduced. Hence, the existence of a travelling wave can possibly explain the difference in the sideband amplitudes observed in figures 4 and 5. Unfortunately it is not possible to specify the magnitudes of the polarization components H^{p}_{0i}, which yield the line shapes for every direction of the magnetic field. From the asymmetry of the sidebands with respect to the π component we estimate a ratio for travelling and standing field amplitudes of $H^{p}_{0i}/H^{a}_{0i}=0{\cdot}5$.

One of the assumptions leading to equations (5) and (8) describing the observed spectra is harmonic modulation of the microwave amplitude, which implies amplitudes of the secular motion much smaller than the distance between two nodes or antinodes of the standing field.

Eventually, splitting of the $\sigma_{\pm}$ carrier resonances at field directions along (1, 0, 1) finds an explanation beyond this model. It is generated by a 50 Hz magnetic ac field emitted from the power supply of the Kr^{+} ion laser, which is placed in the (1, 0, 1) direction with respect to the trap.

Figure 6 shows the observed line shapes for the magnetic field pointing in all (i, j, k) directions $(i, j, k=0, \pm 1)$; it is clearly recognized that changes of the field orientation drastically influence the observed spectra.

6. Conclusions

Microwave spectra of stored ion clouds have been investigated and it was found that the orientation of an externally applied magnetic field with respect to the polarization axis of the applied microwave field leads to drastically varying line shapes. In particular, the amplitude of the motional sidebands behaves differently to that expected from the Zeeman components of the hfs transition. This can be explained by a combination of amplitude modulation in the spatially varying field and a phase modulation in the travelling wave part of the microwave field. Simple arguments based on the assumption of amplitude and phase modulation already suffice to explain the observed spectra and the line shapes. A more detailed analysis, however, would have to solve the difficult problem of finding the spatial pattern of the standing wave field determined by the boundary conditions given by the trap's hyperbolic surfaces.

As far as frequency standard applications are concerned, it is certainly advantageous to operate under conditions which allow the observation of a narrow resonance at the centre frequency without the motional sidebands present (see figure 5, (1, 0, 1) direction). Thus, any shifts and broadenings induced by possibly asymmetric motional sidebands are completely avoided.

Downloaded By: [University of Sao Paulo] At: 21:45 3 March 2010

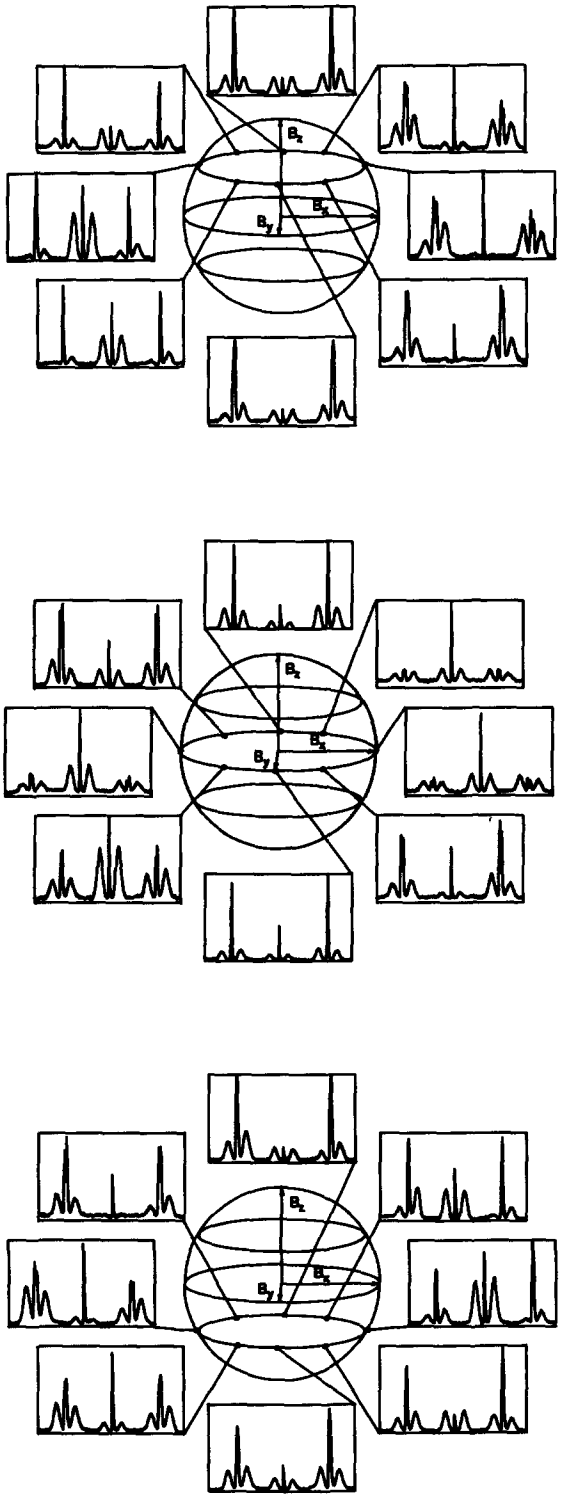

Figure 6. Spectra of the hfs transition components for all (i, j, k) magnetic field orientations $(i, j, k = 0, \pm 1)$.

Downloaded By: [Universisty of Sao Paulo] At: 21:45 3 March 2010

Acknowledgments

The authors wish to thank Professor P. E. Toschek for fruitful discussions. This experiment was supported by the Deutsche Forschungsgemeinschaft.

References

[1] SCHUESSLER, H. A., FORTSON, E. N., and DEHMELT, H. G., 1969, *Phys. Rev.*, **187,** 5.
[2] BLATT, R., and WERTH, G., 1982, *Phys. Rev.* A, **25,** 1476; BLATT, R., SCHNATZ, H., and WERTH, G., 1983, *Z. Phys.* A, **312,** 143.
[3] DICKE, R. H., 1953, *Phys. Rev.*, **89,** 472.
[4] BOLLINGER, J. J., WINELAND, D. J., ITANO, W. M., and WELLS, J. S., 1983, *Proc. 6th Int. Conf. Laser Spectroscopy*, edited by H. P. Weber and W. Lüthy (Berlin: Springer), p. 168.
[5] JARDINO, M., DESAINTFUSCIEN, M., BARILLET, R., VIENNET, J., PETIT, P., and AUDOIN, C., 1981, *Appl. Phys.*, **24,** 107.
[6] CASDORFF, R., ENDERS, V., BLATT, R., NEUHAUSER, W., and TOSCHEK, P. E., 1991, *Ann. Phys.*, **48,** 41.
[7] BLATT, R., CASDORFF, R., ENDERS, V., NEUHAUSER, W., and TOSCHEK, P. E., 1989, *Proc. 4th Int. Symp. Frequency Standards*, edited by A. De Marchi (Berlin: Springer), p. 306.
[8] PAUL, W., OSBERGHAUS, O., and FISCHER, E., 1958, *Forschungsberichte des Wirtschafts- und Verkehrsministeriums Nordrhein-Westfalen Nr. 415* (Cologne: Westdeutscher Verlag); FISCHER, E., 1959, *Z. Physik*, **156,** 1.
[9] DEHMELT, H. G., 1967, *Adv. atom. molec. Phys.*, **3,** 52.
[10] VEDEL, F., ANDRÉ, J., VEDEL, M., and BRINCOURT, G., 1983, *Phys. Rev.* A, **27,** 2321.
[11] CUTLER, L. S., FLORY, C. A., GIFFARD, R. P., and MCGUIRE, M. D., 1986, *Appl. Phys.* B, **39,** 251.
[12] MEIS, C., DESAINTFUSCIEN, M., and JARDINO, M., 1988, *Appl. Phys.* B, **45,** 59.
[13] BLATT, R., ZOLLER, P., HOLZMÜLLER, G., and SIEMERS, I., 1986, *Z. Phys.* D, **4,** 121; SIEMERS, I., BLATT, R., SAUTER, TH., and NEUHAUSER, W., 1988, *Phys. Rev.* A, **38,** 5121.
[14] LI, G. Z., 1989, *Z. Phys.* D, **14,** 1.
[15] SCHWEBEL, C., MÖLLER, P. A., and PHAM TU MANH, 1975, *Rev. Phys. appl.*, **10,** 227.
[16] MEIS, C., JARDINO, M., GELY, B., and DESAINTFUSCIEN, M., 1989, *Appl. Phys.* B, **48,** 67.
[17] LAKKARAJU, H. S., and SCHUESSLER, H. A., 1982, *J. appl. Phys.*, **53,** 3967.

Downloaded By: [University of Sao Paulo] At: 21:45 3 March 2010